ELSEVIER

International Journal of Mass Spectrometry 12091 (2002) 1–15

International Journal of Mass Spectrometry

www.elsevier.com/locate/ijms

Carbocation rearrangements of trimethylsilyl adducts of saturated acyclic C_5–C_7 ketones in the gas phase

Jennie Kong [a,b], Philip S. Mayer [a], Thomas Hellman Morton [a,*]

[a] *Department of Chemistry, University of California, Riverside, CA 92521-0403, USA*
[b] *Laboratoire des Mécanismes Réactionnels, URA CNRS 1307, Ecole Polytechnique, 91128 Palaiseau, France*

Received 11 October 2001; accepted 10 January 2002

Dedicated to the memory of Pierre Longevialle, "explorateur, pas géographe".

Abstract

Metastable ion decompositions of TMS^+ adducts of all the saturated, acyclic C_5–C_7 ketones and of selected ketone conjugate acid ions are compared. The proportion of ions that result from rearrangement of the carbon skeleton tends to increase with the size of the starting ketone. Parent ions derived from α-branched ketones can be subdivided into pairs that rearrange and decompose via common intermediates. In addition to pathways outlined by previous workers, the present study delineates the involvement of ion–neutral complexes and also presents evidence for 1,4-hydride shift. Inclusion of this latter mechanism accentuates the parallelism between the rearrangements of gaseous TMS^+ adducts and those of protonated ketones in solution. Loss of $(CH_3)_3SiOH$ from TMS^+ adducts occurs primarily via 1,2-shift followed by 1,3-elimination, just as water loss takes place from ketones in superacid solution. In most cases the product from this elimination is an allylic cation, but 1,4-hydride shift appears more likely to produce a cyclopropylcarbinyl ion. Density functional calculations give relative energies of pertinent intermediates, products, and transition states for cationic rearrangements. (Int J Mass Spectrom, in press) © 2002 Published by Elsevier Science B.V.

Keywords: Chemical ionization; Protonated ketones; Allylic cations; MIKE spectra; Collisionally activated decomposition; Metastable ion decomposition; Cyclopropylcarbinyl cations; Hydride transfer transition states; Alkyl transfer transition states

1. Introduction

Silicon electrophiles find many uses in organic chemistry. Species such as trimethylsilyl cation (TMS^+) do not occur as free intermediates in solution [1] but pass from one nucleophile to another in a fashion analogous to Brønsted acid–base reactions. That observation has prompted some investigators to liken TMS^+ to a "bulky proton", especially in its attachment to oxygen lone pairs and the reactions that ensue [2].

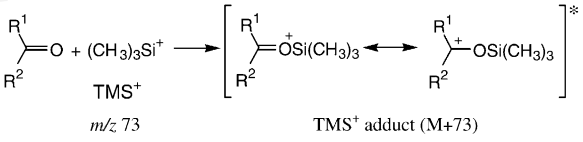

(1)

Free TMS^+ can be readily produced in the gas phase, and it associates with simple ketones with high efficiency, even at low pressures [3]. The ions formed by bimolecular addition to ketones, represented in Eq. (1), tend to persist for many milliseconds in the absence of collisions [4], despite the fact that the association reaction is exothermic by more than 160 kJ mol^{-1}

* Corresponding author. E-mail: morton@citrus.ucr.edu

1387-3806/02/$20.00
PII S1387-3806(02)00576-6

[5,6]. Examination of metastable ion decompositions of TMS^+ adducts of hexanones and their isomers shows that regeneration of TMS^+ constitutes a major unimolecular fragmentation pathway [7]. Therefore, the decomposing ions must have retained virtually all of the energy liberated by the addition reaction that formed them. Consequently, Eq. (1) depicts the initially formed adduct as a vibrationally excited ion, which can survive for microseconds.

Harrison and coworkers [7,8] have reported the metastable decompositions of conjugate acid ions ($M+1$ and $M+2$) and of TMS^+ adducts ($M+73$) of all the saturated, acyclic C_6 ketones. Comparison shows that alkene eliminations occur from both types of parent ions and that the expulsion of $(CH_3)_3SiOH$ from $M+73$ parallels the expulsion of water from $M+1$. Both of those decomposition pathways require that rearrangement take place prior to fragmentation, a result that can be explained in terms of cationic isomerizations. As Eq. (1) portrays, one resonance structure of a TMS^+ adduct places the positive charge on carbon, and migrations of neighboring groups to that electron-deficient center should occur just as they do in $M+1$ ions. This tendency to rearrange limits the utility of TMS^+ adducts for the analytical purpose of distinguishing isomeric ketones.

In strongly acidic solutions, α-branched carbonyl compounds interconvert via pinacol/pinacolone rearrangements (pathway *i*) [9]. Protonated pinacolone, *t*Bu(Me)C=OH^+, scrambles its methyl groups, both in solution and in the gas phase. Among the saturated, acyclic ketones with six carbons, only one pair of interconverting isomers exists, *sec*-butyl methyl ketone and isopropyl ethyl ketone. In the gas phase, H_2 chemical ionization of that pair of isomers shows different fragmentation patterns in the ion source, but identical metastable ion decomposition patterns in the mass-resolved ion kinetic energy (MIKE) spectra of their MH^+ ions [8]. The MIKE spectra of the corresponding TMS^+ adducts appear to exhibit the same trend, though the similarity is not quite so obvious [7]. By examining all the saturated, acyclic C_5–C_7 ketones, we compass the four additional pairs of potentially interconverting TMS^+ adducts of α-branched $C_7H_{14}O$ isomers. Isotopic labeling permits us to assess whether the adducts themselves equilibrate on the 10^{-5} s timescale preceding metastable ion decompositions, or if, instead, they decompose via a set of common intermediates without equilibrating the parent ions.

Four reaction categories (which may operate *seriatim*) have been discussed in this context [7,8]:

(i) reversible 1,2-alkyl and hydrogen shifts (pinacol/pinacolone-type rearrangements);
(ii) 1,3-hydrogen transfer concomitant with cleavage that creates a double bond;
(iii) formation of proton-bound dimer between an alkene and an oxygenated species;
(iv) oxygen migration via formation of an intermediate cyclic oxonium ions.

The metaphor of TMS^+ as a "bulky proton" impels us to examine the TMS^+ adducts ($M+73$) of all 15 saturated, acyclic C_7 ketones and to compare, in appropriate instances, their decompositions with those of the conjugate acid ions. The objectives of this study include exploring whether the above categories constitute accurate descriptions and whether they completely account for the chemistry of conjugate acid and TMS^+ adduct ions, as well as the extent to which these pathways compete with one another. We conclude that category (iii) has to embrace ion–neutral complexes; that at least one additional category (1,4-hydride shift) should be included; and that isotopic labeling reveals more than one route to a given fragment ion.

2. Experimental

Source mass spectra and CAD spectra were recorded on a VG ZAB 2F at UC Riverside. MIKE spectra were performed on the UCR instrument or on a ZAB at the Ecole Polytechnique in Palaiseau that has been specially modified for that purpose by installation of a specially fabricated chemical ionization source. The UCR instrument discriminates against low kinetic energy fragments [10], but the Palaiseau instrument does not. Fragment ion abundances in Ta-

Table 1
Percentages of major metastable ion decomposition products of TMS^+ adduct ions ($M + TMS^+$) from C_5–C_7 ketones

$R^1R^2C{=}O{-}TMS^+$	TMS^+ ($m/z = 73$)	$M + TMS^+ - Me_3SiOH$	$H_2C{=}O{-}TMS^+$ ($m/z = 103$)	$MeCHO{-}TMS^+$ ($m/z = 117$)	$C_3H_6O{-}TMS^+$ ($m/z = 131$)
(**1**) $R^1 = R^2 = Et$	87	<0.5	7	4	<0.5
(**2**) $R^1 = n$Pr, $R^2 = Me$	92	<0.5	4	<0.5	<0.5
(**3**) $R^1 = i$Pr, $R^2 = Me$	96	<0.5	<0.5	<0.5	<0.5
(**4**) $R^1 = n$Bu, $R^2 = Me$	78	5	6	9	<0.5
(**5**) $R^1 = n$Pr, $R^2 = Et$	76	4	8	2	8
(**6**) $R^1 = i$Pr, $R^2 = Et$	61	12	7	16	3
(**7**) $R^1 = s$Bu, $R^2 = Me$	54	14	9	21	3
(**8**) $R^1 = i$Bu, $R^2 = Me$	43	4	4	42	8
(**9**) $R^1 = t$Bu, $R^2 = Me$	86	14	<0.5	<0.5	<0.5
(**10**) $R^1 = R^2 = n$Pr	64	6	10	2	7
(**11**) $R^1 = R^2 = i$Pr	5	4	2	83	4
(**12**) $R^1 = i$PrCH(CH_3), $R^2 = Me$	6	3	1	84	3
(**13**) $R^1 = i$Pr, $R^2 = n$Pr	39	15	8	28	7
(**14**) $R^1 = n$PrCH(CH_3), $R^2 = Me$	40	16	7	29	6
(**15**) $R^1 = Et_2CH$, $R^2 = Me$	39	19	7	13	15
(**16**) $R^1 = s$Bu, $R^2 = Et$	31	21	7	15	20
(**17**) $R^1 = t$Bu, $R^2 = Et$	45	22	1	13	18
(**18**) $R^1 = t$Am, $R^2 = Me$	33	26	1	17	21
(**19**) $R^1 = t$BuCH_2, $R^2 = Me$	5	3	<0.5	2	82
(**20**) $R^1 = n$Bu, $R^2 = Et$	72	5	8	2	11
(**21**) $R^1 = s$BuCH_2, $R^2 = Me$	23	10	3	48	17
(**22**) $R^1 = i$Bu, $R^2 = Et$	28	5	7	1	53
(**23**) $R^1 = i$BuCH_2, $R^2 = Me$	42	46	3	8	1
(**24**) $R^1 = CH_3(CH_2)_4$, $R^2 = Me$	73	7	6	12	<0.5

bles 1 and 2 are based on peak areas measured on the Palaiseau instrument.

Ketones for this study were either purchased commercially or synthesized by conventional methods, including base-catalyzed isotopic exchange with D_2O in the case of α-deuterated compounds. $(CH_3CD_2)_2CHCOCH_3$ was synthesized by Georges Sozzi using an established procedure [11]. MD^+ ions were produced by chemical ionization of α-perdeuterated ketones with D_2O. TMS^+ adducts were formed in the ion source by electron impact on a mixture of hexamethyldisilane and the appropriate ketone under chemical ionization conditions. Because hexamethyldisilane exhibits an intense $m/z = 131$ fragment ion ($M - 15$) as well as an appreciable ion at $m/z = 117$, it was not in general possible to observe the major products of the ion–molecule reactions between TMS^+ and ketones in the ion source. However, in the case of the TMS^+ adduct of $(CH_3CD_2)_2CDCOCD_3$ (**15**-α,β-d_8) it was possible to

Table 2
Metastable ion decompositions via pathway *iii* relative to competing pathways to the same structures, as revealed by deuterium substitution

Parent ion	Me_3SiOH loss	Me_3SiOD loss	$m/z = 104$	$m/z = 105$
$(EtCD_2)_2C{=}O{-}TMS^+$ (**10**-α-d_4)	55	31	29	100
$Me_2CD(EtCD_2)C{=}O{-}TMS^+$ (**13**-α-d_3)	95	77	<0.5	100
$(MeCD_2)_2CH(Me)C{=}O{-}TMS^+$ (**15**-β-d_4)	35	100	43	24
nPrCD$_2$(MeCD$_2$)C=O–TMS$^+$ (**20**-α-d_5)	59	17	21	100
iBuCD$_2$(CD$_3$)C=O–TMS$^+$ (**23**-α-d_5)	100	<0.5	3	<0.5
nBuCD$_2$(CD$_3$)C=O–TMS$^+$ (**24**-α-d_5)	100	6	22	79

resolve the $CD_3CD{=}O{-}TMS^+$ product ($m/z = 121$) from the isobaric $M - 1$ ion of the starting material.

Computation of experimental ratios of overlapping peaks in the MIKE spectra of deuterated compounds was performed by fitting peaks with Gaussians using the commercial IgorPro software. Values for translational kinetic energy releases ($T_{0.5}$) were determined by fitting observed peakshapes to Gaussians using IgorPro software version 3.03 (WaveMetrics, Inc., Lake Oswego, OR) and are reported to the nearest 0.005 V. Density functional theory (DFT) computations of ion structures from first principles were performed using the commercial GAUSSIAN98 code, with geometry optimizations performed at the B3LYP/6-31G** level. Basis set superposition error of 18 kJ mol^{-1} was estimated by counterpoise for the association of TMS^+ with $(CH_3CH_2)_2CHCOCH_3$ to make **15**. Zero-point energies and vibrational entropies were calculated using unscaled harmonic frequencies computed at B3LYP/6-31G**.

3. Results

The TMS^+ adducts of all the saturated, acyclic C_5–C_7 ketones were examined using MIKE spectroscopy. Table 1 summarizes relative intensities of the most abundant products from metastable ion decompositions: TMS^+ ($m/z = 73$); $M + 73 - Me_3SiOH$; and the most prominent alkene expulsions (m/z = 103, 117, and 131). The results for the C_6 ketones are close to the proportions tabulated by Bosma and Harrison [7]. Out of the 15 C_7 ketones, 9 exhibit TMS^+ ($m/z = 73$) as the most intense peak in the MIKE spectra of their TMS^+ adducts. Of the remaining 6, the TMS^+ adduct of isoamyl methyl ketone (**23**) prefers to eliminate Me_3SiOH, while the other five preferentially eliminate alkene, including the four β-branched isomers. Two of the singly β-branched isomers have hydrogen at a tertiary center. These isomers are homologues of isobutyl methyl ketone (**8**, R = R′ = H in Eq. (2)), which has been shown to expel alkene via 1,3-hydrogen shift (pathway *ii*). This is illustrated by Eq. (2), where the homologues correspond to R = CH_3, R′ = H (**21**) and to R = H, R′ = CH_3 (**22**). Their most prominent peaks come from the

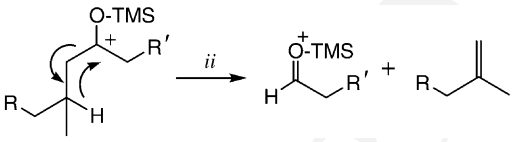

(2)

eliminations expected on the basis of Eq. (2), m/z = 117 and 131, respectively. The third C_7 ketone that has only β-branching, neopentyl methyl ketone, does not possess a β-hydrogen, and its TMS^+ adduct must therefore expel alkene by other pathways.

3.1. Neopentyl methyl ketone

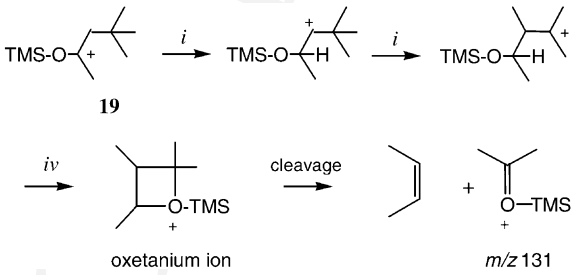

(3)

Different pathways to a given product can be envisaged, based on the reaction categories (i)–(iv) listed above. The predominant ion from the TMS^+ adduct of neopentyl methyl ketone (4,4-dimethyl-2-pentanone, **19**) corresponds to the TMS^+ adduct of acetone ($m/z = 131$). One can draw at least three mechanisms to rationalize this fragmentation. Eq. (3) depicts a series of 1,2-shifts (pathway *i*). Eq. (3) would predict that the deuterium labeled ketone $(CH_3)_3CCD_2COCD_3$ (**19**-α-d_5) should also yield $m/z = 131$, with all of the label contained in the expelled neutral. An alternative mechanism would suppose that rapid 1,2-shifts (pathway *i*) randomize all four methyl groups, such that both $m/z = 131$ (unlabeled) and $m/z = 134$ (one CD_3-group) ions are produced.

Eq. (4) depicts a third mechanism, in which a simple cleavage forms *tert*-butyl cation bound to

the TMS–ether of acetone enol (pathway *iii*). Following Bosma and Harrison [7], the intermediate is drawn as a proton-bound dimer. As will be discussed below in the context of the conjugate acid of $(CH_3)_3CCD_2COCD_3$, this intermediate is probably better viewed as an ion–neutral complex. Regardless of how the intermediate is represented, Eq. (4) predicts that all of the deuterium label

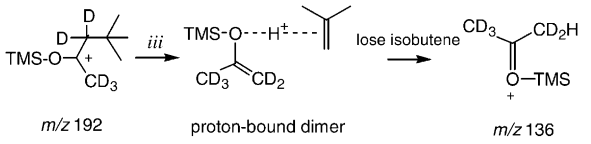

(4)

should be retained by the ion, yielding $m/z = 136$. Experimentally, the TMS^+ adduct of $(CH_3)_3CCD_2CO$-CD_3 produces $m/z = 136$ and 131 in a ratio of 66:1, with no observable $m/z = 134$. Therefore, we conclude that Eq. (4) predominates, with Eq. (3) operating to a very small extent.

3.2. Isoamyl methyl ketone vs. linear heptanones

Eqs. (2) and (4) summarize the effects of β-branching. We now inquire whether more distal branching has an effect, by comparing the TMS^+ adducts of isoamyl methyl ketone (5-methyl-2-hexanone, **23**) and its linear isomer *n*-pentyl methyl ketone (2-heptanone, **24**). These two isomeric ions show marked differences. Nearly, three-quarters of the ions from the linear ketone decompose via TMS^+ expulsion. The major evidence for skeletal rearrangement in that system comes from the formation of $H_2C{=}O{-}TMS^+$. The α-pentadeuterated analogue forms $D_2C{=}O{-}TMS^+$, which can be rationalized in terms of the skeletal rearrangement portrayed in Eq. (5). The labeling experiment does not tell whether the expelled neutral alkene is 1-hexene (via transfer of a methyl hydrogen, pathway *iii*) or 2- or 3-hexene. The other two ions that come from **24**, which are included in Eq. (5), can be rationalized without invoking skeletal rearrangement.

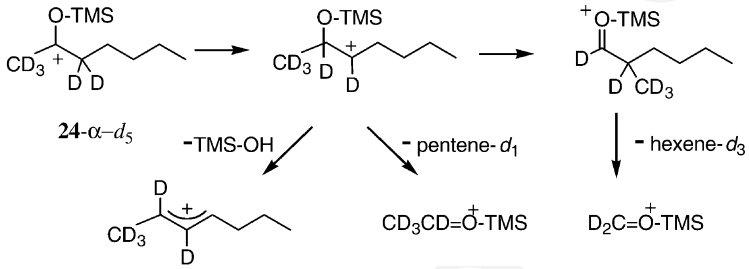

(5)

By contrast, almost half of the decomposing TMS^+ adduct of isoamyl methyl ketone loses Me_3SiOH, as does its α-pentadeuterated analogue (**23**-α-d_5). It would be hard to explain why this branched isomer should give so much more Me_3SiOH loss than does the TMS^+ adduct of any other saturated ketone, if the mechanism were the same as portrayed for the linear isomer in Eq. (5). We therefore put forth the hypothesis depicted in Eq. (6): namely, a 1,4-hydride shift that forms the tertiary cationic center in the isomeric cation **25**. The same type of 1,4-hydride shift has been invoked to account for the unimolecular isomerization of protonated $(CH_3)_2CHCH_2CH_2COCH_3$ in superacid solutions [9]. In support of the notion of a 1,4-hydride shift, Table 2 shows that TMS^+ adducts of the perdeuterated linear heptanones (**10**-α-d_4, **20**-α-d_4, and **24**-α-d_5) lose some Me_3SiOD in addition to Me_3SiOH, while no Me_3SiOD loss can be detected from **23**-α-d_5. Furthermore, the TMS^+ adducts of the α-perdeuterated ketones **13**-α-d_3 and **24**-α-d_5 give $CH_3CD{=}O{-}TMS^+$ and $CD_3CD{=}O{-}TMS^+$, respectively, as the only trimethylsilylated acetaldehyde ions. These ions come from initial 1,2-shift, as exemplified in Eq. (5). Metastable ion decomposition of **23**-α-d_5 gives a 55:45 mixture of $CD_3CD{=}O{-}TMS^+$ and $CD_3CH{=}O{-}TMS^+$, showing that shift from a more distal position is competing with 1,2-shift. A theoretical treatment of Eq. (6) is

presented in Section 4.

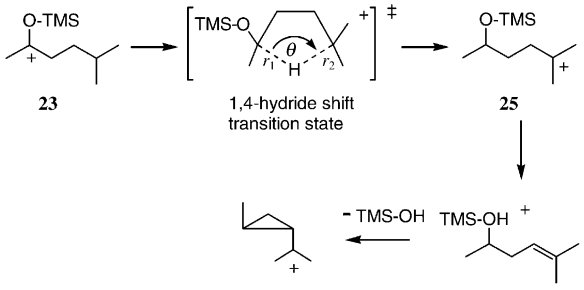

(6)

3.3. 3-Pentyl methyl ketone and sec-butyl ethyl ketone

TMS^+ adducts of the other 10 $C_7H_{14}O$ ketones tend to expel alkene largely via pinacol/pinacolone-type rearrangements (pathway *i*). The TMS^+ adducts of the eight α-branched ketones subdivide into four pairs of interconverting isomers, illustrated by Eqs. (7)–(10), as revealed by similarities in their metastable ion decomposition patterns. Labeling experiments (described below) suggest that the parent ions do not equilibrate completely, but rather that their metastable ion decompositions take place via sets of common intermediates.

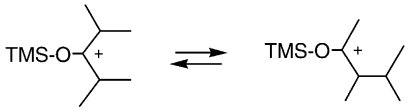

11 **12** (7)

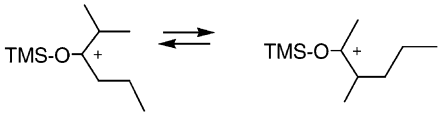

13 **14** (8)

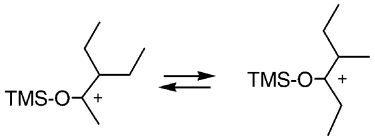

15 **16** (9)

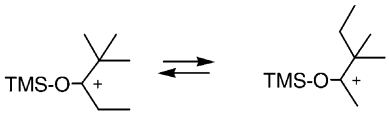

17 **18** (10)

If the proportion of TMS^+ is neglected, the ratios of the other fragment ions are virtually the same for the TMS^+ adducts of 3-pentyl methyl ketone (3-ethyl-2-pentanone, **15**) and *sec*-butyl ethyl ketone (4-methyl-3-hexanone, **16**), m/z = 97:103:117:131:145 = 1:0.37 ± 0.02:0.72 ± 0.01:0.88 ± 0.06:0.27 ± 0.02 (where the uncertainties indicate the spread between **15** and **16**). The same parallelism is to be found in the α-branched C_6 ions **6** and **7**, as previously reported and here confirmed [7]. This suggests a bifurcation of the metastable ion decomposition pathway, with one population of ions expelling TMS^+, while a separate population interconverts among a set of common intermediates via pathway *i* prior to decomposition.

The TMS^+ adducts of diisopropyl ketone (2,4-dimethyl-3-pentanone, **11**) and *sec*-isoamyl methyl ketone (3,4-dimethyl-2-pentanone, **12**) exhibit very little TMS^+ and have virtually identical fragment ion distributions. This pair is discussed at greater length below. Likewise, the TMS^+ adducts of isopropyl *n*-propyl ketone (2-methyl-3-hexanone, **13**) and 2-pentyl methyl ketone (3-methyl-2-hexanone, **14**) display the same metastable ion decomposition patterns. Finally, if the abundance of TMS^+ is neglected, the ratios of rearrangement ions from the TMS^+ adducts of the two α-branched *gem*-dimethyl pentanones—*tert*-butyl methyl ketone (2,2-dimethyl-3-pentanone, **17**) and *tert*-amyl methyl ketone (3,3-dimethyl-2-pentanone, **18**)—are nearly the same, indicating that this pair of structures also pass through a set of common intermediates.

The distribution of label in the ions from the TMS^+ adduct of the β-d_4 analogue of **15** $(CH_3CD_2)_2CHCO\text{-}CH_3$ shows that the steps drawn in Scheme 1 take place. As Table 2 summarizes, loss of Me_3SiOD prevails over loss of Me_3SiOH by a factor of 3:1, suggesting that the parent ion rearranges via a

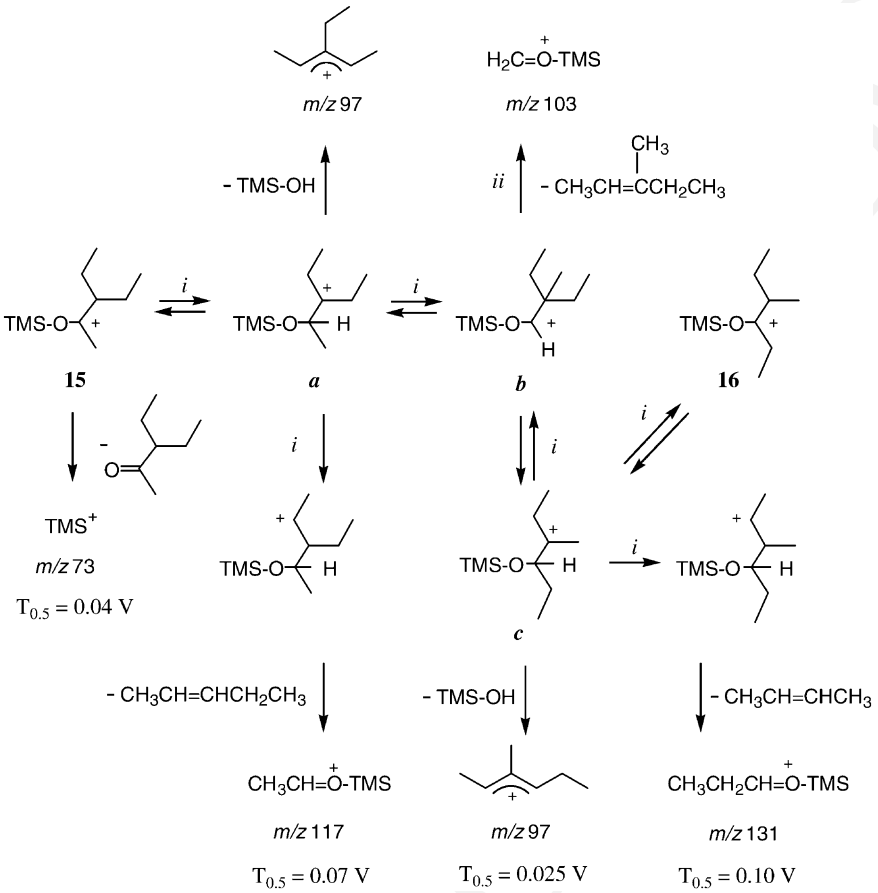

Scheme 1.

1,2-hydrogen shift (pathway *i*) to structure ***a*** and can then undergo a 1,3-elimination to form an allylic ion. This result agrees with the mechanism for Me_3SiOH loss drawn in Eq. (5) for a linear isomer. Structure ***a*** very likely undergoes a second 1,2-hydrogen shift to give an ion that easily expels 2-pentene to form $CH_3CH{=}O{-}TMS^+$, which does not contain any deuterium from the labeled ethyl groups. Alternatively, structure ***a*** can shift a methyl (pathway *i* once more) to give structure ***b***. Vicinal elimination from ***b*** (pathway *ii*) yields $DCH{=}O{-}TMS^+$ (m/z = 104) from the d_4 parent ion. Finally, ***b*** can shift an ethyl to give structure ***c***, which interconverts with the TMS^+ adduct of 4-methyl-3-hexanone. Structure ***c*** can also shift hydrogen to give an ion from which facile elimination of 2-butene produces the TMS^+ adduct of propionaldehyde (m/z = 133, if one starts from $(CH_3CD_2)_2CHCOCH_3$). Structure ***c*** can also expel Me_3SiOH (Me_3SiOD in the case of the β-d_4 analogue). Metastable ion decompositions of the TMS^+ adducts of the α-d_4 analogue of **15**, $(CH_3CH_2)_2CDCOCD_3$ (for which the most abundant rearrangement ions occur at m/z = 121 and 132) and the α,β-d_8 analogue $(CH_3CD_2)_2CDCOCD_3$ (for which the most abundant rearrangement ions occur at m/z = 121 and 134) confirm the pathways for expulsion of 2-pentene and of 2-butene represented in Scheme 1. The presence of $CD_3CD{=}O{-}TMS^+$ (m/z = 121) in the source mass spectrum of the α,β-d_8 analogue of **15** (with an intensity roughly 4%

of the TMS^+ adduct at $m/z = 195$) suggests that rearrangements via structures ***a***–***c*** can compete with Me_3Si^+ expulsion, even when the parent ion contains all the internal energy liberated by the addition of TMS^+ to the ketone.

Scheme 1 depicts two types of alkene elimination: elimination via 1,3-hydrogen transfer (pathway *ii*, such as forms $m/z = 103$) vs. sequential 1,2-shifts (pathway *i*, as forms $m/z = 117$ and 131). As indicated by Eq. (2) above, pathway *ii* has been well documented in the expulsion of isobutene-d_2 from the TMS^+ adduct of $CD_3COCD_2CH(CH_3)_2$ (**8**-α-d_5) [7], a result that we have reproduced. We conclude that hydride shift from a methane group prevails whenever there is branching in the alkyl chain: 1,2-shift for α-branched ketones, 1,3-shift for β-branched ketones, and 1,4-shift for γ-branched ketones. Section 4 treats Scheme 1 theoretically.

We note, parenthetically, that **15** and **16** are the only branched ketone adducts that yield ≥4% of $m/z = 145$ (corresponding to elimination of propene). The only isomer that produces a greater abundance of $m/z = 145$ is the TMS^+ adduct of di-*n*-propyl ketone (4-heptanone, **10**), for which expulsion of propene constitutes 10% of the metastable ion decomposition. The α-d_4 analogue of **10**, $(CH_3CH_2CD_2)_2C{=}O{-}TMS^+$, expels propene-$d_1$, demonstrating that a succession of two 1,2-hydride shifts takes place. The result for **15**-β-d_4 shows that more complicated rearrangements must be occurring in the branched system, since it expels propene-d_4, propene-d_3, and propene-d_2 in a ratio of approximately 2:1:1.

3.4. *sec*-Isoamyl methyl ketone and diisopropyl ketone

How do pathways *i* and *ii* compete when there is both α-branching and β-branching? A *sec*-isoamyl group branches at both positions, and expulsion of C_5H_{10} dominates the metastable ion decompositions of the TMS^+ adduct of *sec*-isoamyl methyl ketone (3,4-dimethyl-2-pentanone, **12**). The deuterated analogue illustrated in Scheme 2 therefore provides a measure of the competition. For the decompositions shown in Scheme 2, pathway *ii* directly from the parent ion should incorporate the tertiary D in the expelled neutral, while pathway *i* from ***d*** should retain that label in the ion. Interpreting the data becomes somewhat complicated, because interconversion of **11** and **12** scrambles the CD_3 group with an unlabeled methyl, as Scheme 2 summarizes. The tertiary D and the tertiary H, however, do not transpose when **12** interchanges with **11**, so that $CD_3CD{=}O{-}TMS^+$ ($m/z = 121$) can arise only via pathway *i*, and $CD_3CH{=}O{-}TMS^+$ ($m/z = 120$) can arise only via pathway *ii* (unless some alternative rearrangement is also taking place). The majority of ions incorporate the tertiary D, implying that the parent ion interconverts with intermediate ***d*** much more rapidly than it goes all the way to **11**. We estimate the ratio of pathway *i* to pathway *ii* as equal to the intensity of $m/z = 121$ relative to $m/z = 120$, 3.5:1.

The TMS^+ adduct of diisopropyl ketone (2,4-dimethyl-3-pentanone, **11**) gives a pattern virtually identical to that of **12**. The predominance of $CH_3CH{=}O{-}TMS^+$ here means that the vast majority of the decomposing ions rearrange to intermediate ***d*** before dissociating. A small proportion of the TMS^+ adducts of both **11** and **12** (2% of the decomposing ions) eliminate propene to yield $m/z = 145$. The TMS^+ adduct of labeled diisopropyl ketone $[(CH_3)_2CD]_2CO$ (**11**-α-d_2) expels propene-d_1, implying that this elimination operates via pathway *ii*. The result of the labeling experiment of **12** informs us that, while **11** and **12** decompose via a common set of intermediates, the parent ions do not equilibrate completely on the microsecond timescale preceding their metastable ion decompositions.

3.5. Conjugate acid ions

Comparison of the TMS^+ adducts with protonated parent ions reveals important aspects of both. In strongly acidic solutions, saturated ketones rearrange and dehydrate to form allylic cations [9,12]. The same reaction appears to take place in the gas phase, since loss of water occurs prominently in the metastable

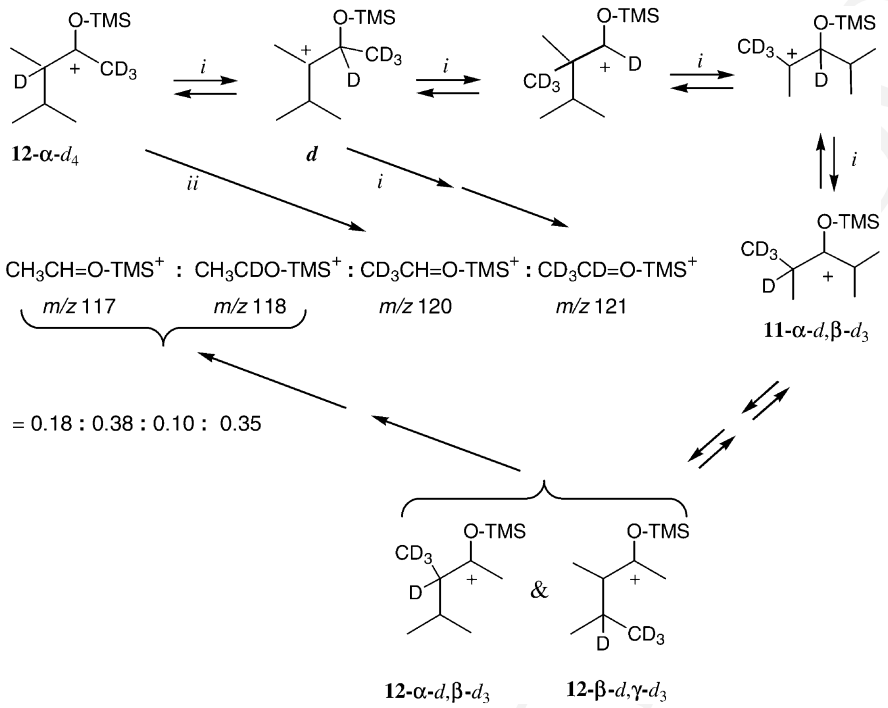

Scheme 2.

ion decompositions of many protonated ketones [13]. Table 3 surveys the collisionally activated decomposition (CAD) spectra of the MH^+–H_2O ions ($m/z = 97$) from $C_7H_{14}O$ ketones in the ion source. Everyone gives rise to a different fragmentation pattern. Thus, it is apparent that, unlike the TMS^+ adducts that survive to decompose in the second field-free region, prompt rearrangement and elimination of water from the MH^+ ions of α-branched ketones do not take place via sets of common intermediates.

Metastable ion decompositions of MD^+ ions from selected α-deuterated ketones reinforce the conclusion that isoamyl methyl ketone behaves differently from its isomers. Some branched MD^+ ions display little or no metastable water loss (e.g., those from diisopropyl ketone and neopentyl methyl ketone). In the case of diisopropyl ketone, it is a curious coincidence that the $M^{\bullet+}$ and the MH^+ ions both exhibit prominent loss of a 44 amu neutral. On the one hand, labeling the α-positions reveals that the $M^{\bullet+}$ ion loses propane, since $[(CH_3)_2CD]_2C{=}O^{\bullet+}$ expels a 46 amu neutral.

Table 3
Relative intensities of the major fragments in the CAD spectra of $m/z = 97$ from the ion source produced by CH_4 chemical ionization of $C_7H_{14}O$ ketones

$R^1R^2C{=}O$	*m/z*			
	55	69	81	82
$R^1 = R^2 = n$Pr	100	24	26	16
$R^1 = R^2 = i$Pr	86	100	73	13
$R^1 = i$PrCH(CH_3), R^2 = Me	100	42	52	3
$R^1 = i$Pr, $R^2 = n$Pr	100	55	74	59
$R^1 = n$PrCH(CH_3), R^2 = Me	100	79	92	29
$R^1 = Et_2CH$, R^2 = Me	100	18	24	13
$R^1 = s$Bu, R^2 = Et	100	36	32	6
$R^1 = t$Bu, R^2 = Et	73	73	100	20
$R^1 = t$Am, R^2 = Me	74	44	100	13
$R^1 = t$BuCH$_2$, R^2 = Me	20	21	56	100
$R^1 = n$Bu, R^2 = Et	100	34	24	9
$R^1 = s$BuCH$_2$, R^2 = Me	100	76	60	25
$R^1 = i$Bu, R^2 = Et	100	20	22	8
$R^1 = i$BuCH$_2$, R^2 = Me	30	32	100	32
$R^1 = CH_3(CH_2)_4$, R^2 = Me	100	49	4	51

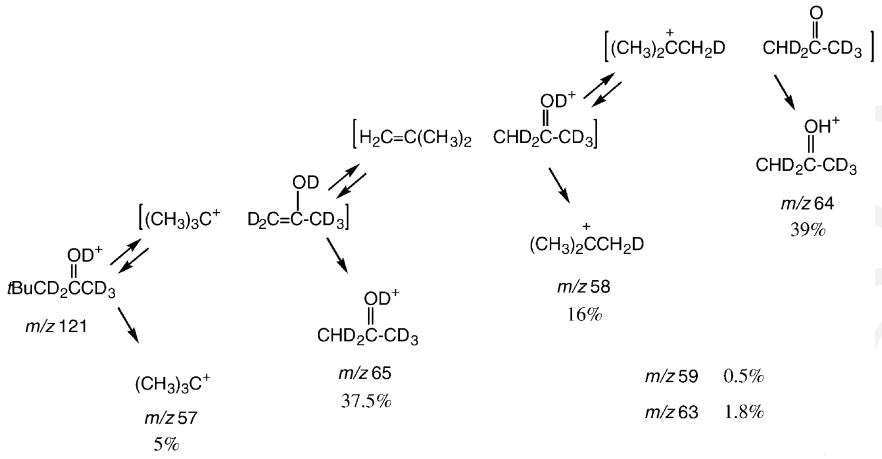

Scheme 3.

On the other hand, $[(CH_3)_2CD]_2C{=}OH^{\bullet+}$ expels a 45 amu neutral, demonstrating that this corresponds to loss of acetaldehyde via a rearrangement passing through a structure analogous to intermediate ***d***.

The metastable ion decompositions of the MD^+ ion from $(CH_3)_3CCD_2COCD_3$ show that H/D exchange takes place between the two fragments created by a simple bond cleavage that is analogous to the one drawn in Eq. (4) above. The resulting ions correspond to protonated acetone and *tert*-butyl cation. If the intermediate were a proton-bound dimer, as Eq. (4) portrays for the TMS^+ adduct, then one would predict the hydrogen that is shared between the two fragments to end up in the observed ion. The experimental data contradict this expectation. The sequence of steps depicted in Scheme 3 depicts how, instead, most of the isotopic interchange very likely occurs through a sequence of ion–neutral complexes. Production of $m/z = 59$ and 63 indicates that exchange can continue further, but their low abundances show that transfer between two carbons does not occur to any great extent. By analogy, we conclude that the intermediate shown in Eq. (4) is better represented as an ion–neutral complex than as a proton-bound dimer.

Water loss is the most abundant decomposition from the MD^+ ions of isopropyl *n*-propyl and isoamyl methyl ketone, as well as from the linear heptanones. The MD^+ ions from the three α-perdeuterated linear heptanones and from α-perdeuterated isopropyl *n*-propyl ketone all display mixtures of MD^+–H_2O, MD^+–HOD, and MD^+–D_2O, with MD^+–HOD being the most abundant, as listed in Table 4. By contrast, MD^+ ions from *i*$BuCD_2COCD_3$ produce almost no MD^+–D_2O. This result is consistent with a 1,4-hydride shift followed by reversible transfer of a

Table 4
Abundances of isotopic water loss from MD^+ ions of selected α-perdeuterated ketones (relative to loss of HOD)

	MD^+–H_2O	MD^+–HOD	MD^+–D_2O
$CD_3COCD_2CH_2CH_2CH_2CH_3$	25	100	8.5
$CH_3CD_2COCD_2CH_2CH_2CH_3$	15.5	100	39
$CH_3CH_2CD_2COCD_2CH_2CH_3$	13.5	100	36
$(CH_3)_2CDCOCD_2CH_2CH_3$	29.5	100	37
$(CH_3)_2CHCH_2CD_2COCD_3$	42	100	1.5

proton from carbon to oxygen, as Eq. (11) illustrates.

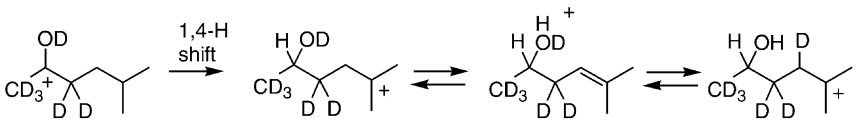

(11)

4. Discussion

TMS^+ attaches to simple ketones at low pressures with rate constants ≥70% of the collision rate. The high efficiency of bimolecular attachment has been ascribed to spontaneous emission of IR from the adduct ion [3]. Radiative association of this sort, however, cannot provide the only explanation for long lived TMS^+ adduct ions, since many of them regenerate TMS^+ in their MIKE spectra (a reaction that would be thermochemically impossible if the parent ions had lost internal energy after formation). We therefore surmise that a fraction of the TMS^+ adduct ions must form with high rotational angular momenta and owe their long lifetimes to a substantial centrifugal barrier for dissociation. Thus, we infer at least two populations of ions that undergo metastable ion decompositions: one population having enough energy to return to TMS^+ plus neutral ketone and the other having lower energy content, which gives rise to the bulk of the observed rearrangements.

The experiments reported here explore the extent to which pathways *i–iv* listed at the beginning of this paper can account for the rearrangements of TMS^+ adduct and conjugate acid ions derived from the saturated acyclic C_5–C_7 ketones. Since none of the C_6 ketones can branch further than the β-position relative to the carbonyl group, the option of 1,4-hydride transfer has not previously been explored in the gas phase. Metastable ion decompositions of the conjugate acid and TMS^+ adduct ions from isoamyl methyl ketone provide evidence for 1,4-hydride transfer, which must be added to the list of cationic rearrangements. The rearrangement processes reported for carbonyl compounds in strong acid solution [9,12,14] accord with behavior seen in the gas phase. Products resulting from 1,4-hydride transfer will be discussed in greater detail below.

Bond cleavage in a gaseous ion does not always lead to immediate separation of the two fragments. Formation of a transient proton-bound dimer has been listed among the dissociation mechanisms (pathway *iii* listed at the beginning of this paper). For TMS^+ adduct ions, that pathway cannot be distinguished from formation of an ion–neutral complex. However, the labeling result for the MD^+ ion from tBuCD$_2$COCD$_3$ summarized in Scheme 3 indicates that the bridging hydrogen does not remain isolated, as would be anticipated on the basis of the directed valence implicit in the description of a proton-bound dimer. Instead, it undergoes exchange, a process that characterizes ion–neutral complexes [15–18]. Pursuing the analogy of TMS^+ as a "bulky proton", pathway *iii* should be expanded to include the formation of ion–neutral complexes.

The similarities of the decomposition patterns of TMS^+ adducts of α-branched ketones shown in Eqs. (7)–(10) can be interpreted in two ways. Either the pairs of isomeric ions equilibrate prior to dissociation, or else they decompose via a common set of intermediates without completely equilibrating. The quantitative results summarized in Scheme 2 imply that this second, more restrictive description applies. If ion **12** equilibrated completely with **11** prior to expelling alkene, one should have expected nearly equal proportions of $m/z = 121$ and 117 among the metastable ion decomposition products. Since the ratio of those ions is approximately 2:1, equilibration of parent ion structures cannot have gone to completion. This result is to be compared with the interconversion of the protonated analogues in solution, represented in Eq. (12), which has an equilibrium constant of $K_{eq} = 3$ and a rate constant of $k_f + k_b = 3 \times 10^{-4}\ s^{-1}$

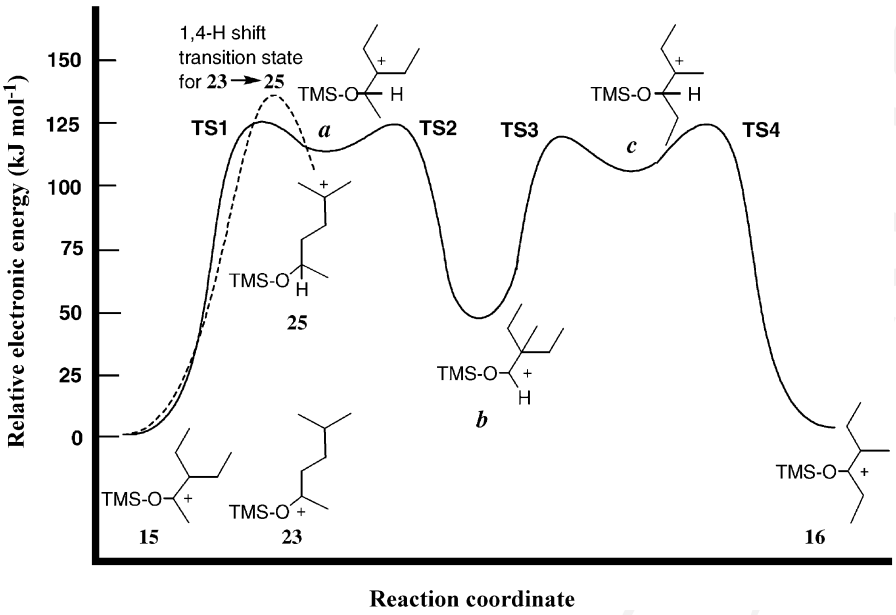

Fig. 1. Electronic energy profile (B3LYP/6-31G**) for interconversion of **15** with **16** via intermediates ***a***, ***b***, and ***c***, based on DFT stationary points. Dashed curve corresponds to the 1,4-hydride shift in **23** shown in the top line of Eq. (6): **23** and **15** have the same heats of formation (within 1 kJ mol^{-1}), while isomerization of **23** to a *tert*-alkyl cation is 12 kJ mol^{-1} less endothermic than the isomerization of **15** to intermediate ***a***.

for equilibration of the isomers [9].

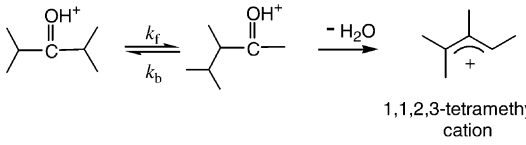

(12)

We have probed the potential energy surface corresponding to Scheme 1 using DFT. The solid curve in Fig. 1 shows a profile corresponding to the electronic energies of ions **15** and **16**, the common intermediates ***a*–*c*** through which they pass, and the four transition states **TS1**–**4**. The four barriers have nearly the same height, and the energy profile along the reaction coordinate appears nearly symmetrical. DFT thermochemical results listed in Table 5 indicate that the barriers lie much lower than the energy of TMS^+ plus neutral ketone, so that interconversion among the intermediates is plausible even when the adduct ion has lost internal energy via emission of radiation or by inelastic collisions. It is worth noting that 1,2-shifts of hydride (**TS1**), of methyl (**TS2**), and of ethyl (**TS3**) all have nearly the same activation energies and entropies. If we compare **TS1** with the barrier for 1,2-hydride transfer in lower homologue **7** (the TMS^+ adduct of *sec*-butyl methyl ketone) we find that the latter has a ΔH° that is lower by 8 kJ mol^{-1}. The experimental estimate [7] of the activation barrier for the isomerization drawn in Eq. (13) (en route to equilibration of *sec*-butyl methyl ketone with isopropyl ethyl ketone) in solution at 300 K, $\Delta G^\circ \approx 100$ kJ mol^{-1}, is not far from the value we calculate for 1,2-hydride transfer in **7**, $\Delta G^\circ = 109$ kJ mol^{-1}.

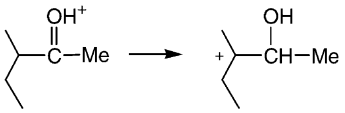

(13)

We now turn to the products of ion decomposition. In solution, both of the protonated ketones in Eq. (12) dehydrate to produce 1,1,2,3-tetramethylallyl cation,

Table 5
B3LYP/6-31G** relative energies (including BSSE) and vibrational entropies (using unscaled vibrational frequencies) of selected cationic $C_7H_{14}O$–TMS systems

	ΔH_{rel} (kJ mol^{-1})	S_{vib} (J K^{-1} mol^{-1})
$Et_2CHCOMe + TMS^+$	0	191
$Et_2CHC(Me)O–TMS^+$ (**15**)	−208	282
*s*BuC(Et)O–TMS$^+$ (**16**)	−202	274
*i*BuCH_2C(Me)O–TMS$^+$ (**23**)	−209	280
$Me_2CCH_2CH(Me)O–TMS^+$ (**25**)	−105	287
1,4-Hydride shift TS (**23** → **25**)	−78	250
TS1	−92	269
Intermediate ***a***	−99	270
TS2	−87	270
Intermediate ***b***	−160	269
TS3	−94	270
Intermediate ***c***	−107	281
$Me_2C=O–TMS^+$ + *trans*-2-butene	−159	218
$EtCH=O–TMS^+$ + *trans*-2-butene	−115	218
$MeCH=O–TMS^+$ + *trans*-2-pentene	−109	208
$H_2C=O–TMS^+$ + 3-methyl-2-pentene	−33	207
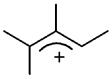 + TMS-OH	−132	210
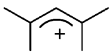 + TMS-OH	−149	202
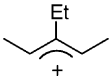 + TMS-OH	−104	205
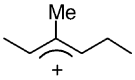 + TMS-OH	−108	223
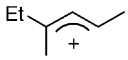 + TMS-OH	−128	201
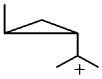 + TMS-OH	−99	193

as depicted. A 1,2-hydride shift in $(i\text{Pr})_2C=OH^+$ followed by a 1,2-elimination would have produced the symmetrically substituted 1,1,3,3-tetramethylallyl cation, which is much more stable (as Table 5 summarizes). Hence, 1,3-elimination must be kinetically favored in solution. Dehydration of the two protonated ketones in the ion source following methane CI produces different sets of $C_7H_{13}^+$ structures, as the CAD spectra summarized in Table 3 attest. Clearly, complete equilibration of the protonated ketones does not precede water loss in the CI source.

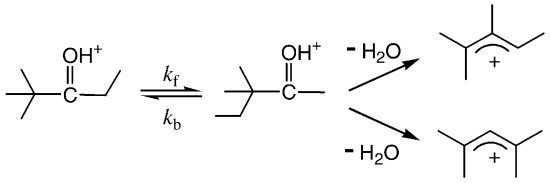

(14)

Similarly, the protonated *tert*-alkyl ketones in Eq. (14) equilibrate in solution, with a solvent-dependent rate constant in the range $k_f + k_b = (0.5–2.3) \times 10^{-4}\,s^{-1}$ at 310 K [9]. The dehydration products are also solvent-dependent. Under the some superacidic

conditions both ketones yield 1,1,2,3-tetramethylallyl cation, just as do the ketone conjugate acids in Eq. (12), while other media lead to a mixture containing the more stable 1,1,3,3-tetramethylallyl cation. In any event, the gas phase dehydration product distributions are not identical in the ion source.

The products of Me_3SiOH loss in the metastable ion decompositions of TMS^+ adducts exhibit a preference for 1,3-elimination, as the labeling results in Table 2 imply and as Eq. (5) illustrates. The set of common intermediates ***a***–***c*** in Scheme 1 can produce two different allylic cations via 1,3-elimination, depending on whether this elimination takes place from ***a*** or ***c***. The hypothesis of common intermediates does not demand that ***a*** and ***c*** equilibrate completely prior to decomposition, so it is possible that precursors **15** and **16** produce different proportions of the three ethyl dimethylallyl cations listed in Table 5. The labeling results in Table 2 do not distinguish among those possibilities. The most stable of these allylic cations, however, would have to arise via a 1,2-elimination from intermediate ***c***. Since 1,3-elimination has been documented for protonated ketones in solution, as Eq. (12) portrays, the less stable ethyl dimethylallyl cations should be kinetically favored if the same preference operates in the gas phase.

Fig. 1 compares the transition state for 1,4-hydride transfer in **23** with 1,2-transfer in **15** and **16**. As the dashed curve indicates, isomerization to the *tert*-alkyl cation **25** (as drawn in Eq. (6)) is less endothermic in the case of **23** than is the isomerization of **15** to intermediate ***a*** or **16** to intermediate ***c***. However, the calculated barrier for 1,4-hydride transfer is higher. Brouwer and Kiffen [14] have compared experimental rates of unimolecular 1,2-, 1,3-, and 1,4-hydride transfer within protonated aldehydes in solution and conclude that 1,4-transfer is slower than 1,2- and faster than 1,3-hydride transfer, a result consistent with our calculations. The structure calculated for the 1,4-shift transition state ($r_1 = 1.155$ Å, $r_2 = 1.95$ Å, $\theta = 118^\circ$) suggests that it occurs later than the 1,2-shift transition state **TS1** (where the bond lengths correspond to r_1 and are 1.21 and 1.59 Å, respectively).

Eq. (6) draws a cyclopropylcarbinyl cation as the ultimate product that results from 1,4-hydride transfer in **23** followed by elimination of Me_3SiOH from **25**. As Table 5 shows, this cation is not very much less stable than isomeric allylic cations. Indeed, this cyclopropylcarbinyl cation is sufficiently long-lived in solution that the circular dichroism spectrum has been reported for a single enantiomer [19]. The inference that the cyclopropylcarbinyl cation forms from **23** is based, in part, on the dehydration of protonated isoamyl methyl ether, iBuCH$_2$C(Me)OH$^+$. As Table 3 summarizes, the CAD of that $C_7H_{13}^+$ ion differs markedly from those produced by methane CI of the other 14 $C_7H_{14}O$ ketones. There are 27 possible allylic cation structures with this formula (if *cis–trans* and stereoisomerism are neglected). It seems likely that the $C_7H_{13}^+$ mixtures from methane CI of the $C_7H_{14}O$ ketones include all of them. Nevertheless, the pattern from the dehydration product of iBuCH$_2$C(Me)OH$^+$ cannot be fitted as a linear combination of the other patterns, which suggests that it contains a $C_7H_{13}^+$ isomer with a unique structure.

5. Conclusions

The present work provides evidence that rearrangements of ketone conjugate acids and TMS^+ adducts in the gas phase mirror the isomerization and dehydration pathways of protonated ketones in solution: 1,2-alkyl and hydrogen shifts, formation of double bonds by 1,3-elimination, and 1,4-hydride shift. Oxygen transposition, while detectable, occurs to a very slight extent compared with competing pathways, just as has been reported in solution. 1,2-Alkyl and hydrogen shifts, which correspond to pinacol/pinacolone rearrangements, lead to sets of common intermediates between pairs of α-branched ions but do not completely equilibrate their structures before decomposition. 1,3-Elimination is kinetically favored over 1,2-elimination in the production of allylic ions, just as has been inferred from solution phase studies. 1,3-Hydrogen shift (concomitant with elimination of alkene) obtains in β-branched ions,

but 1,2-hydrogen shift prevails in ions that have both α- and β-branching. Hydrogen shift from tertiary carbon occurs even from distal positions; however, 1,4-hydride shift is calculated to have a higher barrier than 1,2-shift, even when the tertiary carbocation produced by the former is more stable. Available evidence suggests the elimination that follows 1,4-shift yields a stable cyclopropylcarbinyl cation in preference to a thermodynamically preferred allylic cation.

Acknowledgements

The authors are grateful to Henri Audier, in whose laboratory most of the MIKE spectra were recorded. This work was supported by NSF grant CHE 9983610.

References

[1] C.A. Reed, Acc. Chem. Res. 31 (1998) 325–332.
[2] J.R. Hwu, J.M. Wetzel, J. Org. Chem. 50 (1985) 3946–3948.
[3] Y. Lin, D.P. Ridge, B. Munson, Org. Mass Spectrom. 26 (1991) 550–558.
[4] I.A. Blair, J.H. Bowie, Aust. J. Chem. 32 (1979) 1389–1393.
[5] M.L. Hendewerk, D.A. Weil, T.L. Stone, M.R. Ellenberger, W.E. Farneth, D.A. Dixon, J. Am. Chem. Soc. 104 (1982) 1794–1799.
[6] H. Basch, T. Hoz, S. Hoz, J. Phys. Chem. A 103 (1999) 6458–6467.
[7] N.L. Bosma, A.G. Harrison, Rapid Commun. Mass Spectrom. 8 (1994) 886–890.
[8] M. Weiss, R.A. Crombie, A.G. Harrison, Org. Mass Spectrom. 22 (1987) 216–223.
[9] D.M. Brouwer, J.A. van Doorn, Recl. Trav. Chim. Pays Bas 90 (1971) 1010–1026.
[10] X. Li, A.G. Harrison, J. Am. Chem. Soc. 115 (1993) 6327–6332.
[11] J.H. Bowie, M.B. Stringer, G.J. Corrie, J. Chem. Soc., Perkin Trans. 2 (1986) 1821–1825.
[12] D.M. Brouwer, J.A. van Doorn, Recl. Trav. Chim. Pays Bas 91 (1972) 261–272.
[13] U.I. Záhorscky, Org. Mass Spectrom. 17 (1982) 253–260.
[14] D.M. Brouwer, A.A. Kiffen, Recl. Trav. Chim. Pays Bas 92 (1973) 906–914.
[15] R.D. Bowen, Acc. Chem. Res. 24 (1991) 364–371.
[16] T.H. Morton, Org. Mass Spectrom. 27 (1992) 353–368.
[17] P. Longevialle, Mass Spectrom. Rev. 11 (1992) 157–192.
[18] D.J. McAdoo, T.H. Morton, Acc. Chem. Res. 26 (1993) 295–302.
[19] R.G. Ghirardelli, J. Am. Chem. Soc. 95 (1973) 4987–4990.